Int. J. Electrochem. Sci., 10 **(2015)** 1529 - 1542

International Journal of ELECTROCHEMICAL SCIENCE
www.electrochemsci.org

Cis/Trans Geometric Effect on the Electro-Optical Properties and Electron Injection in Indole-Based Squaraine Sensitizers: Quantum Chemical Investigations

Abdullah M. Asiri[1,2], *Sultan A. H. Al-Horaibi*[1], *Ahmad Irfan*[3,*], *Salem A. Basaif*[1], *Reda M. El-Shishtawy*[1]

[1] Chemistry Department, Faculty of Science, King Abdulaziz University, P.O. Box 80203, Jeddah 21589, Saudi Arabia
[2] Center of Excellence for Advanced Materials Research, King Abdulaziz University, P.O. Box 80203, Jeddah 21589, Saudi Arabia
[3] Department of Chemistry, Faculty of Science, King Khalid University, Abha 61413, P.O. Box 9004, Saudi Arabia
[*]E-mail: irfaahmad@gmail.com

Received: 31 October 2014 / *Accepted:* 14 December 2014 / *Published:* 30 December 2014

Squaraine dyes gained significant attention as dye-sensitized solar cell (DSSCs) materials. In present study; we have studied the important parameters which influence the performance of DSSCs by considering the TiO_2 clusters as acceptor material. We have investigated the structural, electro-optical and charge transport properties of six indole-based squaraine dyes (Cis-SQ1-SQ3 and Trans-SQ1-SQ3). The ground state geometries have been optimized by using density functional theory (DFT) then excitation energies and oscillator strengths were computed by time-dependent DFT in solvent. We shed light on the frontier molecular orbitals (highest occupied and lowest unoccupied molecular orbitals), electron injection (ΔG^{inject}), relative electron injection (ΔG_r^{inject}), electronic coupling constants ($|V_{RP}|$), light harvesting efficiencies (LHE), short-circuit current density (J_{sc}) and open-circuit voltage (V_{oc}). The ΔG^{inject}, ΔG_r^{inject} and $|V_{RP}|$ of six sensitizers have been compared with some previously studied sensitizers. The effect of donor ($-OCH_3$) and acceptor (-COOH) groups has been investigated and discussed on said properties of interests. The Cis/Trans geometric effect has been studied on the structural parameters, absorption wavelengths, ΔG^{inject}, $|V_{RP}|$, LHE, V_{oc} and factors affecting the J_{sc}. It has been discussed that which geometric isomer would be more favorable to enhance the performance of DSSCs.

Keywords: Solar cells; indole-based squaraine dyes; Density functional theory; Short-circuit current density; Open circuit voltage

1. INTRODUCTION

Nowadays organic compounds gain noteworthy consideration due to low cost, environment friendly, ease to modify chemically and structural flexibility [1-5]. The squaraine dyes are proficient organic materials which are used for multifunctional purposes, e.g. bioimaging application [6], sensors [7] and semiconducting devices such as laser technology [8], organic light emitting diodes (OLEDs) [9], organic field effect transistors (OFETs), and photovoltaic cells [10-12]. Recently, the squaraine dyes are used as dye-sensitized solar cells (DSSCs) [13-15] due to large absorption coefficients in the red and near-infrared [16, 17], improved charge injection and efficiency [18-20]. The H- and J-aggregates of indole-based squaraine dyes (e.g. SQ26) have been studied [21]. Miguel and co-investigators address the femto- to millisecond transient absorption studies of TiO_2 thin films with indole-based squaraine sensitizers and they found that electron injection occurred from squaraine dye to TiO_2 conduction band [21]. Previously, electronic and charge transport properties of metal free sensitizers have been studied by density functional theory (DFT) and it was concluded that superior light harvesting efficiencies (LHE), intra-molecular charge transfer (ICT), electron injection and electronic coupling constants would lead efficient sensitizers [22-28] which was in good agreement with the Wiemer studies [29]. The charge recombination and dye aggregation can leads to lower efficiency [30-33]. Thus we have selected such squaraine dyes having long side chains and acidic ligands, see Fig. 1. It is expected that long side chains would inhibit the recombination while acidic ligands would hamper the aggregation.

Present study deals in depth quantum chemical investigations of six indole-based squaraine dyes (Cis/Trans-SQ1-SQ3, see Fig. 1) with the aim to study the electro-optical properties, electron injection ($\Delta G^{inject.}$), electronic coupling constants ($|V_{RP}|$), light harvesting efficiencies (LHE), short-circuit current densities (J_{sc}) and open-circuit voltages (V_{oc}). The computed properties have been compared with the available theoretical and experimental data. Moreover, the $\Delta G^{inject.}$, $|V_{RP}|$ and LHE have been compared with some previously studied sensitizers. Then the Cis/Trans geometric effect has been discussed on the above mentioned properties.

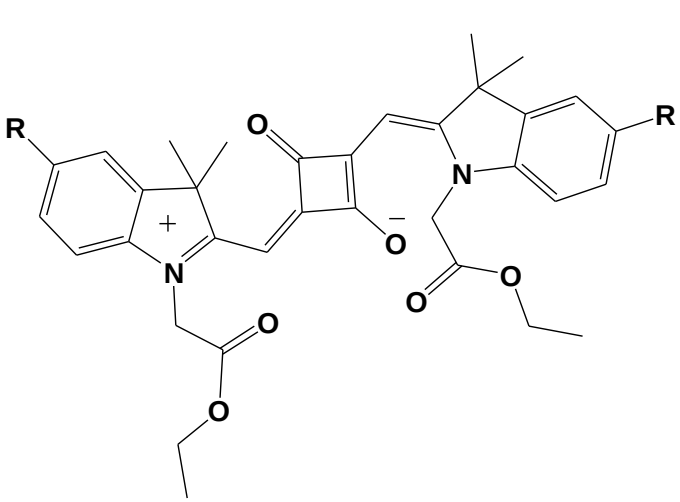

Cis-SQ1, R = H
Cis-SQ2, R = COOH
Cis-SQ3, R = OCH_3

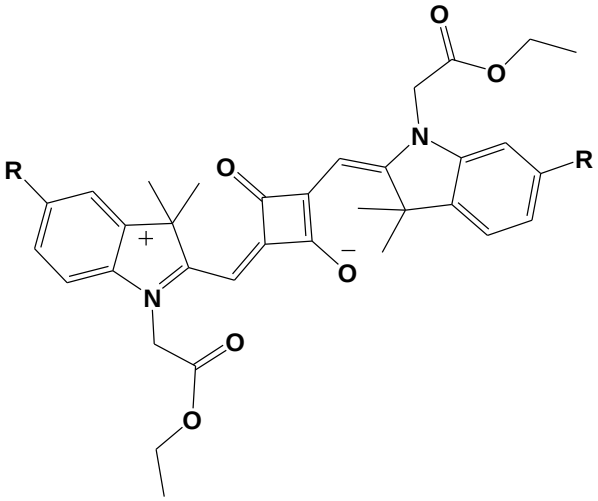

Trans-SQ1, R = H
Trans-SQ2, R = COOH
Trans-SQ3, R = OCH_3

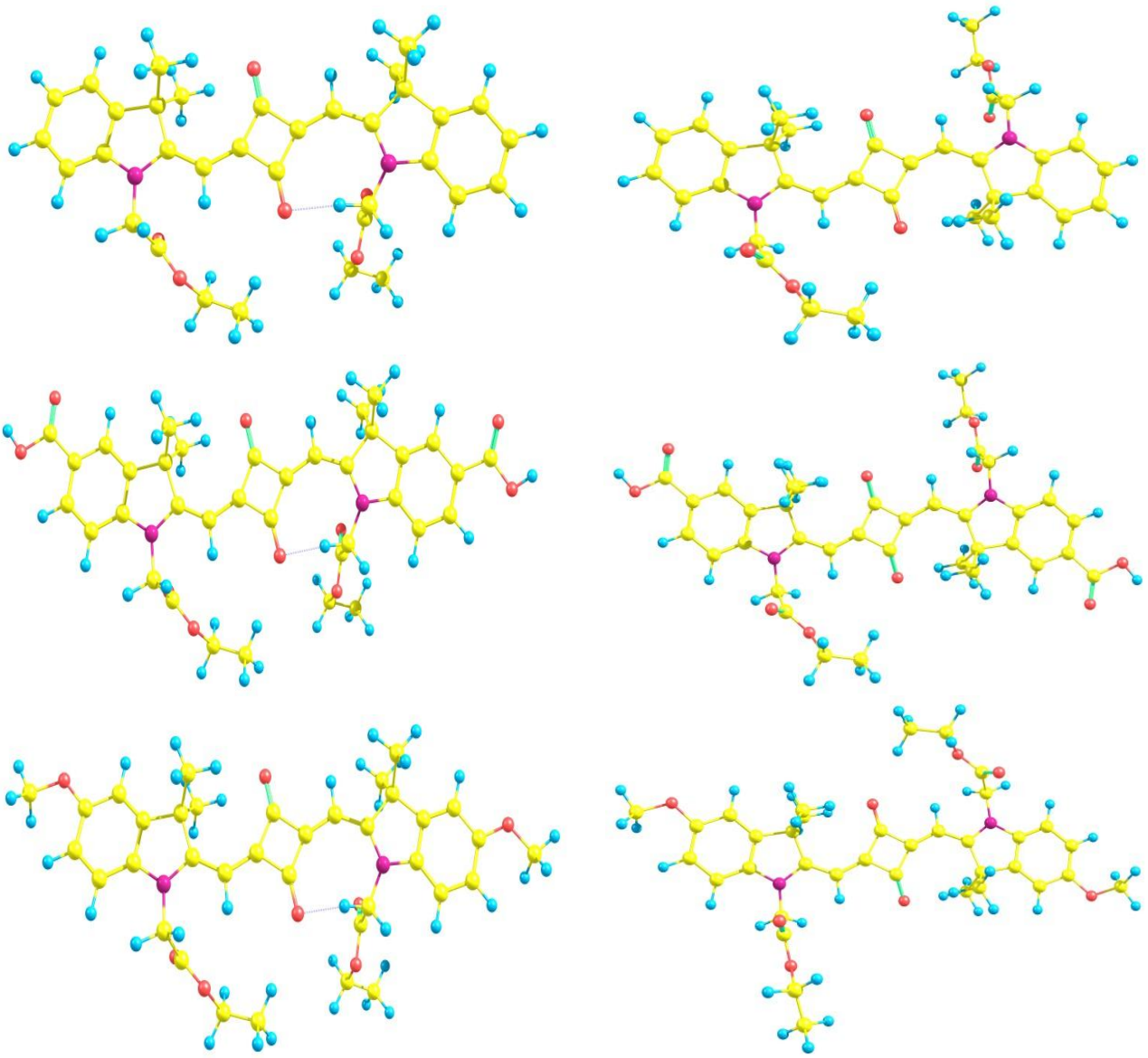

Figure 1. The structures of the indole-based squaraine dyes; Cis (left) Trans (right) investigated in the presented study (schematic (top) and optimized structures (bottom).

In the best of our knowledge, no quantum chemical studies have been carried out on these indole-based squaraine dyes with respect to DSSCs. The paper is structured as follows: Section 2 presents an outline of the DFT and Time Dependent DFT (TDDFT), including the rationale for choosing the hybrid functional and the basis set; Section 3 includes the geometries, frontier molecular orbitals both distribution patterns as well as the energies of highest occupied molecular orbitals (E_{HOMOs}), lowest unoccupied molecular orbitals (E_{LUMOs}), absorption spectra (λ_a), excitation energies, LHE, $|V_{RP}|$ and $\Delta G^{inject.}$ of DSSCs; in Section 4 the major conclusions of the present investigation have been presented.

2. COMPUTATIONAL DETAILS

Numbers of studies have shown that the DFT is reasonable theory which reproduces the experimental results more accurately for small organic compounds [27, 34-46]. There are a number of good DFT functionals; among those B3LYP provides best interpretation [34-37, 46-49]. Previously the absorption wavelengths of hydrazone, azobenzene, anthraquinone, phenylamine and indigo dyes were computed; they found that B3LYP functional is a good approach which reproduces the experimental evidences more precisely [50]. Previously the geometric parameters, electronic, photo-physical and charge transport properties have been calculated by applying the B3LYP and TD-B3LYP functionals [25, 51, 52] and it was showed that these functionals are rational for azo dyes [53, 54], triphenylamine dyes [26], chemosensors [55], phthalocyanines [24], biologically active molecules [56], and oxadiazoles [57]. The electron injection in organic triphenylamine based compounds has been calculated by B3LYP/6-31G** level of theory and it was found that this level of theory is adequate [30, 58]. More recently, B3LYP/6-31G** and PBE0/6-31G** levels of theories have been applied to optimize and shed light on the electronic and charge transport properties of naphtho[2,3-*b*]thiophene. They pointed out that B3LYP/6-31G** level of theory was in good agreement to reproduce the experimental results [59]. The experimental absorption and emission wavelengths of different organic compounds have been reproduced by using the TDDFT [35, 46, 60]. Thus in the present study, the ground state geometries, electronic properties and absorption spectra have been computed at B3LYP/6-31G** and TD-B3LYP/6-31G** levels of theories, respectively.

The rate of electron/charge transfer process from dye to metal oxides can be explained by Marcus theory [61-65],

$$k_{inject.} = |V_{RP}|\, 2/h\, (\pi/\lambda k_B T)1/2 \exp[-(\Delta G_{inject.} - \lambda)2/4\lambda k_B T] \quad (1)$$

In eq. (1), $k_{inject.}$ is the rate constant (in S^{-1}) of the electron injection from dye to metal oxides, k_{BT} is the Boltzmann thermal energy, *h* the Planck's constant, $\Delta G^{inject.}$ the electron injection and λ is the reorganization energy of the system, $|V_{RP}|$ is the electronic coupling constant. The improved $|V_{RP}|$ would lead to enhance the rate constant resulting efficient sensitizer. By Mulliken-Hush formalism, we can calculate the $|V_{RP}|$ [62, 63]. The Hsu et al. calculated $|V_{RP}|$ by half of the injection driving force (ΔE_{RP}) according to eq. 2 [63].

$$|V_{RP}| = \Delta E_{RP}/2 \quad (2)$$

Here ΔE_{RP} can be expressed within Koopmans approximation as

$$\Delta E_{RP} = [E^{dye}_{LUMO} + 2E^{dye}_{HOMO}] - [E^{dye}_{LUMO} + E^{dye}_{HOMO} + E^{TiO_2}_{CB}] \quad (3)$$

where $E^{TiO_2}_{CB}$ is the conduction band edge which is difficult to determine precisely due to highly sensitive to the conditions thus we used experimental value, i.e., $E^{TiO_2}_{CB}$ = -4.0 eV [66-68]. The E^{dye}_{LUMO} corresponds to the reduction potential of the dye (E^{dye}_{RED}) while the HOMO energy is related to the potential of first oxidation (i. e., $-E^{dye}_{HOMO} = E^{dye}_{OX}$) thus eq. (3) can be expressed as,

$$\Delta E_{RP} = [E^{dye}_{HOMO} - E^{TiO_2}_{CB}] = -[E^{dye}_{OX} + E^{TiO_2}_{CB}] \quad (4)$$

The eq. (4) can be rewritten as

$$\Delta E_{RP} = E^{dye}_{0-0} - [2E^{dye}_{OX} + E^{dye}_{RED} + E^{TiO_2}_{CB}] \quad (5)$$

To evaluate the potential of first oxidation of dye's excited and electron injection onto TiO_2 surface, we calculated the free energy change (ΔG^{inject}, in eV) which can be expressed as [67].

$$\Delta G^{inject} = E_{OX}^{dye*} - E_{CB}^{TiO_2} \quad (6)$$

where E_{OX}^{dye*} is the oxidation potential of the dye in the excited state. To calculate the E_{OX}^{dye*} two models can be used [69, 70]. The first entails that the electron injection occurs from the unrelaxed excited state. The excited state oxidation potential can be extracted from the redox potential of the ground state, E_{OX}^{dye} and the vertical transition energy corresponding to the photoinduced ICT,

$$E_{OX}^{dye*} = E_{OX}^{dye} - \lambda_{\max}^{ICT} \quad (7)$$

where $\lambda_{\max}^{ICT}$ is the energy of the ICT. Note that this relation is only valid if the entropy change during the light absorption process can be neglected. Preat and co-authors showed that the $\lambda_{\max}^{ICT}$ can be evaluated during the electronic excitation which is equal to the absorption energy. For the second model, one assumes that electron injection occurs after relaxation. Given this condition, E_{OX}^{dye*} is expressed as [70]:

$$E_{OX}^{dye*} = E_{OX}^{dye} - E_{0-0}^{dye} \quad (8)$$

where E_{0-0}^{dye} is the transition energy between the ground electronic state/ground vibrational state (n=0/v=0) and the first excited electronic state/ground vibrational state (n=1/v=0). This is denoted as 0-0 and is defined as the lowest energy transition". To estimate the 0-0 "absorption" line, both the S_0 (singlet ground state) and the S_1 (first singlet excited state) equilibrium geometries, Q_{S0} and Q_{S1} are required, respectively. Previously electron injection has been observed from unrelaxed excited states in TiO_2 [71] and SnO_2 [72]. Most of the experimentalists assume that electron injection ensues after relaxation but the relative contribution of an ultrafast injection path is not clear. Preat et al. pointed out that the absolute difference between the relaxed and unrelaxed $\Delta G_{inject.}$ is constant, and is of the same order of magnitude than the E_{OX}^{dye} and E_{OX}^{dye*} mean average error [58]. The ΔG^{inject} and E_{OX}^{dye*} have been evaluated using Eqs. (6) and (7).

The LHE of the dye has to be as high as possible to maximize the photocurrent response. The LHE can be expressed as [73]:

$$\mathrm{LHE} = 1 - 10^{-\mathrm{A}} = 1 - 10^{-f} \quad (9)$$

where A (f) is the absorption (oscillator strength) of the dye associated to the $\lambda_{\max}^{ICT}$. The oscillator strength is directly derived from the TDDFT calculations as follow:

$$f = \frac{2}{3}\lambda_{\max}^{\mathrm{ICT}} |\vec{\mu}_{0-\mathrm{ICT}}|^2 \quad (10)$$

where $\mu_{0-\mathrm{ICT}}$ is the dipolar transition moment associated to the electronic excitation. In order to maximize f, both $\lambda_{\max}^{ICT}$ and $\mu_{0-\mathrm{ICT}}$ must be large [74] [75].

The efficiency (η) of solar cells can be determined by using the following equation

$$\eta = FF\frac{V_{oc}J_{sc}}{P_{inc}} \quad (11)$$

where J_{sc} is the short-circuit current density, V_{oc} is the opencircuit photovoltage, FF is the fill factor, and $P_{inc.}$ is the intensity of the incident light. The J_{sc} can be evaluated as

$$J_{sc} = \int_{\lambda} LHE(\lambda)\phi_{injection}\eta_{collection}d\lambda \quad (12)$$

where $\eta_{collection}$ is the charge collection efficiency which is constant. From above equation, we can find that J_{sc} is directly linked with the LHE and $\phi_{injection}$ is electron injection efficiency which is related to ΔG^{inject}. It is revealing that higher LHE and ΔG^{inject} would lead efficient devices [76].

3. RESULTS AND DISCUSSION

3.1. Geometries

We have presented geometrical parameters of six Cis/Trans indole-based squaraine dyes in Table 1. The C_1-N_1, C_3-C_4 bond lengths shortened while C_4-N_1, C_2-C_3 lengthened from Cis-SQ1 to Trans-SQ1. All other selected geometrical parameters of Cis-SQ2/SQ3 and Trans-SQ2/SQ3 compounds are nearly alike, respectively. The C_1-N_1, C_3-C_4 bond lengths shortened while C_2-C_3, C_4-N_1 lengthened in Cis-SQ2 and Cis-SQ3 compared to Cis-SQ1. In Trans-SQ2, the C_1-N_1 bond length shortened compared to Trans-SQ1. The bond lengths lengthening/shortening in Cis forms is larger and more than Trans ones. When –COOH and $–OCH_3$ groups are substituted at –R positions then C_1-N_1, C_3-C_4 usually shortened while C_4-N_1, C_2-C_3 bond distances lengthened than SQ1 in Cis forms. It is might be due to the moderate electron withdrawing groups (2-ethoxy-2-oxoethyl) which are in the same side which influence geometry more than Trans isomers in which 2-ethoxy-2-oxoethyl cancel the effect of each other. Thus in Trans forms geometric variations in SQ2 and SQ3 are smaller than the Cis ones.

Table 1. The geometrical parameters, bond lengths (Å) and bond angles (°) of indole-based squaraine dyes optimized at B3LYP/6-31G** level of theory.

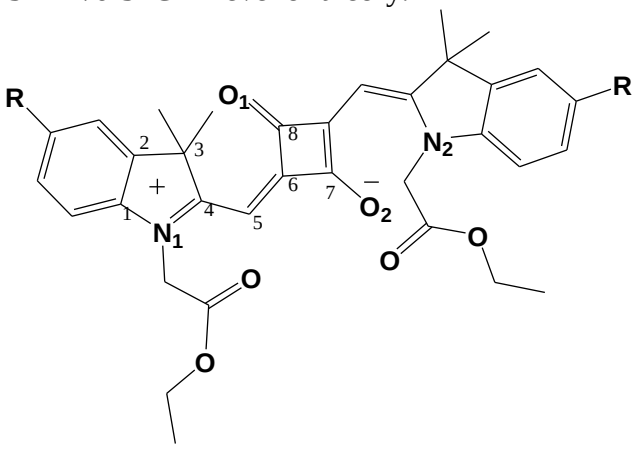

	Cis-SQ1	Cis-SQ2	Cis-SQ3	Trans-SQ1	Trans-SQ2	Trans-SQ3
Bond lengths						
C_1-C_2	1.396	1.401	1.400	1.398	1.401	1.399
C_1-N_1	1.412	1.400	1.409	1.408	1.400	1.409
C_4-N_1	1.368	1.380	1.375	1.376	1.380	1.376
C_2-C_3	1.515	1.520	1.521	1.520	1.521	1.521
C_3-C_4	1.543	1.534	1.536	1.535	1.534	1.537
C_8-O_1	1.230	1.229	1.231	1.232	1.231	1.232
C_7-O_2	1.238	1.237	1.239	1.235	1.234	1.236
Bond angles						
C_1-N_1-C_4	111.76	111.77	111.80	111.77	111.78	111.81
C_2-C_3-C_4	101.44	101.35	101.48	101.46	101.35	101.48
C_4-C_5-C_6	131.97	131.86	132.02	132.01	131.89	132.04
C_6-C_8-O_1	137.31	137.36	137.27	137.36	137.40	137.32
C_6-C_7-O_2	132.70	132.74	132.70	132.83	132.86	132.83

3.2. Frontier molecular orbitals and absorption spectra

In Fig. 2, we have illustrated the charge density distribution patterns of the ground state highest occupied molecular orbitals (HOMOs and HOMOs-1), lowest unoccupied molecular orbitals (LUMOs and LUMOs+1) of six Cis/Trans-SQ1-SQ3 indole-based squaraine dyes. The HOMOs-1 are distributed on the squaraine moieties except in Cis-SQ3 in which indole is also taking part in the formation of HOMO-1. Most of the charge density is disseminated on the entire systems in the formation of the HOMOs and LUMOs. The LUMOs+1 are localized on both of the indole units in Cis/Trans-SQ1 and Cis/Trans-SQ2. While in Cis/Trans-SQ3 only right indole moiety is taking part in the formation of LUMOs+1. The –COOH and carbonyl groups of 2-3-(2-ethoxy-2-oxoethyl) are participating in the formation of LUMOs and LUMOs+1 in Cis/Trans-SQ2 and all other dyes, respectively. The charge density on carbonyl LUMOs and LUMOs+1 is superior in Cis-SQ1-SQ3 than Trans-counterparts.

In Table 2, we have presented the computed HOMOs energies (E_{HOMOs}), LUMOs energies (E_{LUMOs}), LUMOs+1 energies ($E_{LUMOs+1}$) and energy gaps (E_g) of six Cis/Trans-SQ1-SQ3 indole-based squaraine dyes at B3LYP/6-31G** level of theory. Generally, the E_{HOMOs}, E_{LUMOs} and $E_{LUMOs+1}$ decrease in Cis/Trans-SQ2 while increases in Cis/Trans-SQ3 than the Cis/Trans-SQ1 showing that by substituting the electron withdrawing group –COOH usually lower while electron donating group –OCH_3 boost up the energies. The computed E_g of Cis/Trans-SQ2 and Cis/Trans-SQ3 are smaller than Cis/Trans-SQ1 revealing that the absorption spectra of formers would be red shifted. The E_{HOMOs}, E_{LUMOs}, $E_{LUMOs+1}$ and E_g of Cis forms are lower/smaller than the Trans ones. But the effect is not so significant resulting no prominent red shift in the absorption wavelengths of Cis form than Trans ones. The smaller E_g of all the six dyes than dyenitro (2.81 eV) [23] are revealing that DSSCs performance of Cis/Trans sensitizers would be superior than later reference compound. The smaller E_{LUMO} of Cis/Trans-SQ2 than other compounds showed that injected electrons would be more stable and by losing electron the charge transport can't be quenched in prior ones.

The Cis/Trans sensitizers have acidic ligands, e.g. Cis/Trans-SQ2 have –COOH group while Cis/Trans-SQ1 and Cis/Trans-SQ3 carbonyl moieties which are good light harvesting sites as well as would be helpful to anchor with the TiO_2 surface. The acidic ligands would also enhance the solubility in solution and reduce aggregation [77]. It is expected that Cis/Trans-SQ2 would be more stable after anchoring on TiO_2 surface, see the localization of LUMOs on –COOH in Fig. 2. Moreover, acidic ligands would be promising positions to transfer the electrons from dyes to TiO_2 surface. Moreover, long side chains would produce a barrier between holes in the redox couple and electrons in the TiO_2 to hinder recombination.

Table 2. The calculated HOMO energies (E_{HOMO}), LUMO energies (E_{LUMO}), LUMO+1 energies (E_{LUMO+1}), energy gaps (E_g) and absorption wavelengths (λ_a) of indole-based squaraine dyes at B3LYP/6-31G** and TD-B3LYP/6-31G** level of theories, respectively.

	E_{HOMO} (eV)	E_{LUMO} (eV)	E_{LUMO+1} (eV)	E_g (eV)	f	λ_a (nm)	Transition
[a]Dyenitro	-6.42	-3.61	-	2.81	1.323	528	H -> L
Cis-SQ1	-4.64	-2.38	-0.39	2.26	1.714	599	H -> L
Cis-SQ2	-4.95	-2.73	-1.30	2.22	1.890	617	H -> L
Cis-SQ3	-4.44	-2.23	-0.36	2.21	1.837	620	H -> L
Trans-SQ1	-4.61	-2.33	-0.30	2.28	1.730	595	H -> L
Trans-SQ2	-4.91	-2.68	-1.24	2.23	1.868	614	H -> L
Trans-SQ3	-4.41	-2.18	-0.27	2.23	1.855	617	H -> L

[a]Detail can be found in reference [53]

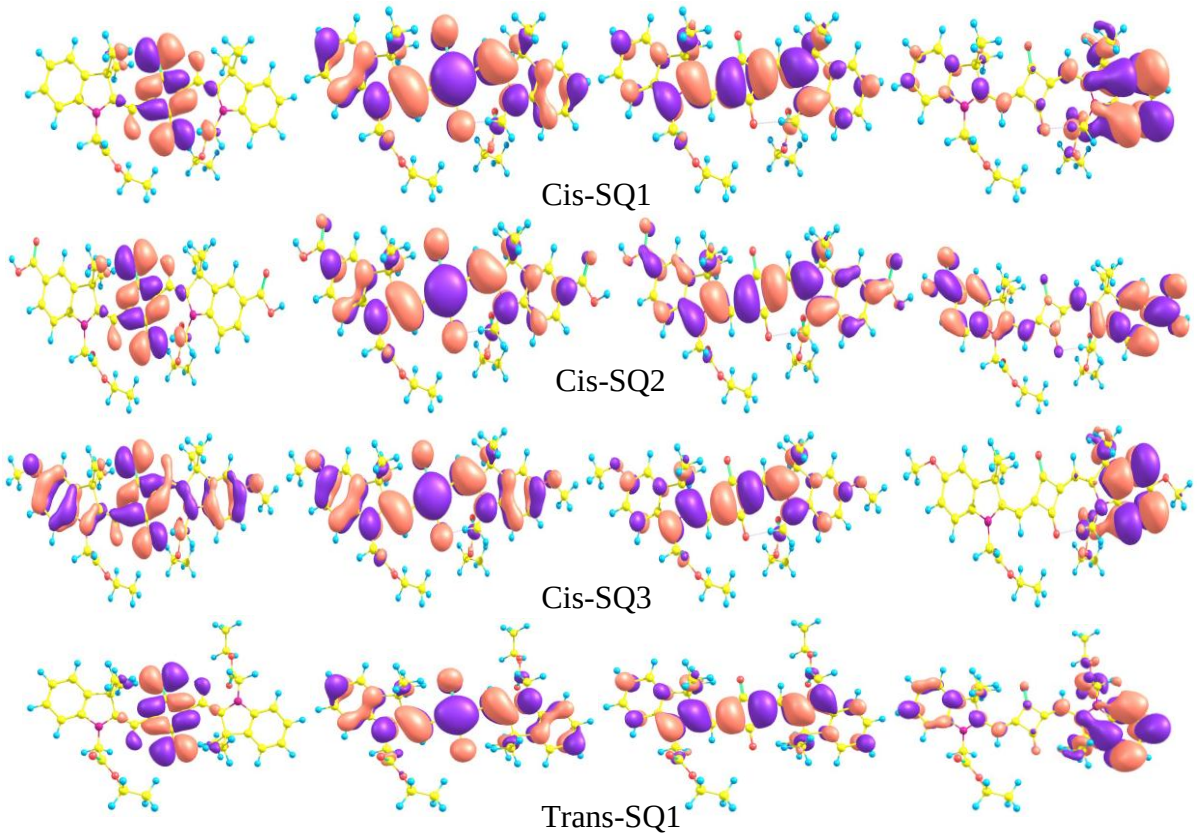

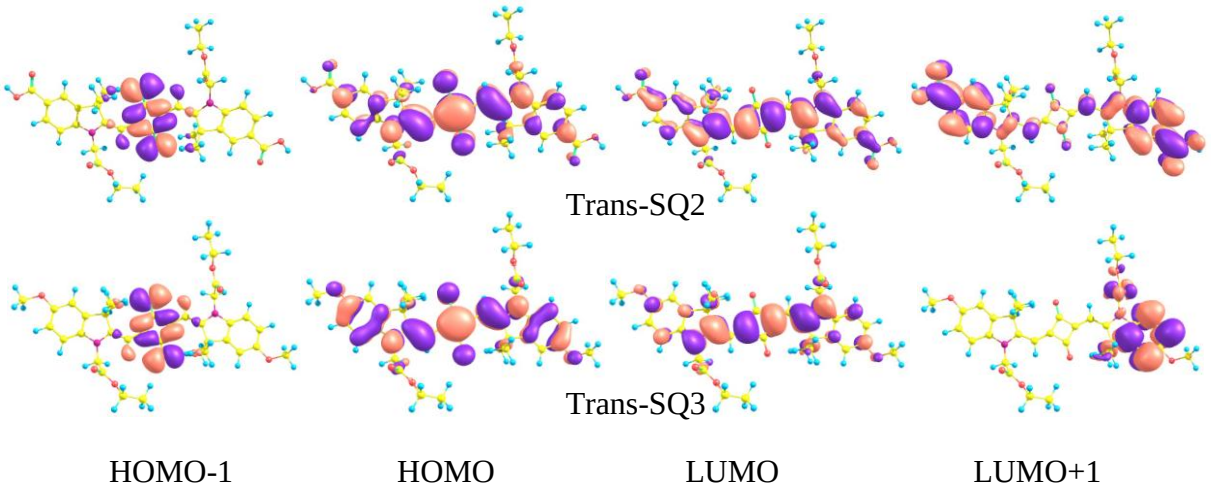

Figure 2. The charge density distribution of the frontier molecular orbitals (0.02 contour value) of indole-based squaraine dyes at B3LYP/6-31G** level of theory.

To validate the level of theory, we have computed the absorption spectra of 2-3-(2-ethoxy-2-oxoethyl)benzo[d]thiazol-2(3H)-ylidene)methyl)-4-((3-(2-ethoxy-2-oxoethyl)benzo[d]thiazol-3-ium-2-yl)methyl-ene)-3-oxocyclobut-1-enolate (BT) which has almost similar structure like studied compounds except "S" has been substituted by -$C(CH_3)_2$ in indole-based squaraine dyes.

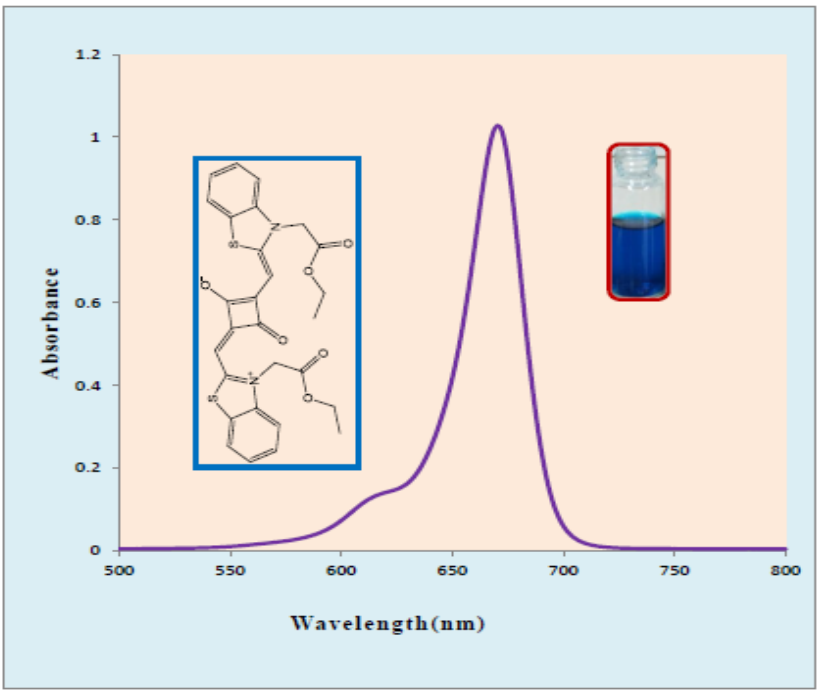

Figure 3. UV-visible spectra (in chloroform , λ max 671 nm) of Dye **(**2-3-(2-ethoxy-2-oxoethyl)benzo[d]thiazol-2(3H)-ylidene)methyl)-4-((3-(2-ethoxy-2-oxoethyl)benzo [d]thiazol-3-ium-2-yl)methyl-ene)-3-oxocyclobut-1-enolate**)**.

The calculated maximum absorption wavelength of BT at TD-B3LYP/6-31G** level of theory in chloroform has been observed 630 nm which is in good agreement with the experimental data, i.e., 671 nm, see Fig. 3. In Table 2, we have tabulated the computed absorption wavelengths (λ_a), oscillator strengths (*f*) and major transitions of Cis/Trans indole-based squaraine sensitizers in chloroform at TD-B3LYP/6-31G** level of theory. The major transitions have been observed from H -> L in all the six indole-based squaraine sensitizers. The calculated λ_a of Cis-SQ1 has been observed 599 nm. The λ_a of Cis-SQ2 and Cis-SQ3, Trans-SQ2 and Trans-SQ3 are being 18, 21, 15 and 18 nm red shifted while Trans-SQ1 4 nm blue shifted compared to Cis-SQ1. The Cis-SQ1-SQ3 sensitizers are red shifted than Trans-SQ1-SQ3 but the geometric effect is not so significant absorption wavelengths.

3.3. Short-circuit current density (J_{sc})

In Table 3, we have presented the ΔG^{inject}, E_{OX}^{dye}, E_{OX}^{dye*}, λ_{max}^{ICT}, LHE, $|V_{RP}|$ and ΔG_r^{inject} of indole-based squaraine sensitizers. The negative calculated values of ΔG^{inject} showing that dye's excited state would lies above the conduction band edge of TiO_2 resulting favorable condition for electron injection. It can be seen from eq. 12 that there are two major factors which influence and enhance the J_{sc}, i.e., LHE and Φ_{inject}. By improving the LHE, photocurrent response can boost up in DSSCs. The $\Phi_{inject.}$ is related to the ΔG^{inject} and here we have discussed both of the factors, i.e., $\Delta G^{inject.}$ and LHE. The ΔG^{inject} of Cis-SQ1, Cis-SQ2, Cis-SQ3, Trans-SQ1, Trans-SQ2, and Trans-SQ3 are 3.18, 2.45, 3.43, 3.28, 2.51 and 3.51 times superior to dyenitro. The major transitions correspond HOMO -> LUMO in all the six Cis/Trans indole-based squaraine sensitizers. The $|V_{RP}|$ and ΔG_r^{inject} in Cis/Trans-SQ3 and Cis/Trans-SQ2 increased and decreased compared to Cis/Trans-SQ1 revealing that $-OCH_3$ at the –R positions improve while –COOH group reduce them. Additionally, we did not observe the significant geometric effect from Cis to Trans forms on the $|V_{RP}|$ and ΔG_r^{inject}.

The values of $|V_{RP}|$ and ΔG^{inject} for different hydrazones and azo sensitizers have been previously computed at TD-B3LYP/6-31G* level of theory, e.g. dyenitro (-0.39 and 0.195 eV), 2-{4-[2-p-chlorobenzylidenehydrazino]phenyl}-ethylene-1,1,2-tricarbonitrile and 2-{4-[2-p-bromobenzylidenehydrazino]phenyl}ethylene-1,1,2-tricarbonitrile (-0.53 and 0.265 eV), respectively [53], 3-(4-methyl-phenylazo)-6-(4-nitro-phenylazo)-2,5,7-triaminopyrazolo[1,5-a]pyrimidine (-1.19 and 0.53 eV) [78]. The calculated $|V_{RP}|$ and ΔG_r^{inject} values of indole-based squaraine sensitizers are revealing electron injection in these dye would be superior to above mentioned hydrazone and azo dyes.

Table 3. The ΔG^{inject}, ΔG_r^{inject}, oxidation potential, light harvesting efficiencies (LHE), $|V_{RP}|$ of investigated sensitizers in chloroform at TD-B3LYP/6-31G** level of theory.

System	ΔG^{inject} (eV)	E_{OX}^{dye} (eV)	E_{OX}^{dye*} (eV)	λ_{max}^{ICT} (eV)	*f*	*LHE*	ΔG_r^{inject} (eV)	$\|V_{RP}\|$ (eV)
[a]Dyenitro	-0.39	5.96	3.61	2.35	1.319	0.9520	1.00	0.195
Cis-SQ1	-1.24	4.83	2.76	2.07	1.714	0.9807	3.18	0.620

Cis-SQ2	-0.96	5.05	3.04	2.01	1.890	0.9871	2.45	0.480
Cis-SQ3	-1.34	4.66	2.66	2.00	1.837	0.9854	3.43	0.667
Trans-SQ1	-1.28	4.80	2.72	2.08	1.730	0.9814	3.28	0.640
Trans-SQ2	-0.98	5.04	3.02	2.02	1.868	0.9864	2.51	0.490
Trans-SQ3	-1.37	4.64	2.63	2.01	1.855	0.9860	3.51	0.685

ΔG_r^{inject}= relative electron injection ΔG^{inject}(dye)/ ΔG^{inject}(Dyenitro)

[a]Detail can be found in reference [53]

The LHE of six indole-based squaraine dyes are greater than the dyenitro, see Table 3. No significant variation has been observed in LHE by changing the geometries from Cis to Trans forms. The Cis/Trans-SQ2 have superior LHE followed by Cis/Trans-SQ3 as compared to Cis/Trans-SQ1.

The greater LHE and ΔG^{inject} values of six indole-based squaraine sensitizers than dyenitro (0.9520 and -0.39), 2-{4-[2-p-chlorobenzylidenehydrazino]phenyl}-ethylene-1,1,2-tricarbonitrile and 2-{4-[2-p-bromobenzylidenehydrazino]phenyl}ethylene-1,1,2-tricarbonitrile (0.9208 and -0.53), respectively [53]; the azo dye 3-(4-methyl-phenylazo)-6-(4-nitro-phenylazo)-2,5,7-triaminopyrazolo[1,5-a]pyrimidine (0.8732 and -0.86) [78] are illuminating that former sensitizers would be proficient materials for DSSCs.

3.4. Open-circuit voltage (V_{oc})

Generally, open-circuit voltage (V_{oc}) is only measured by experimental means as the relationship among the electronic structure of the dye and these quantities is not clear till now. We can obtain energy relationship according to the sensitized mechanism, single electron and single state approximation as follow:

$$eV_{oc} = E_{LUMO} - E_{CB} \quad (13)$$

Brabec et. al pointed out that the V_{oc} intensely depends on the E_{LUMO} [79]. The larger values of the E_{LUMO} would lead superior V_{oc}. The reduction potential (E_{LUMO}) of the Cis/Trans-SQ2 is greater than the Cis/Trans-SQ1 and Cis/Trans-SQ3 enlightening that V_{oc} of former sensitizers would be higher than later ones. It is anticipated that –COOH groups are most promising sites to transfer the electrons from dyes to TiO_2 surface resulting improved V_{oc}. The larger reduction potential of Cis isomers than Trans ones are displaying that former might have larger V_{oc} but the effect of geometric variation from Cis to Trans is not so significant.

4. CONCLUSIONS

The geometric alteration from Cis to Trans forms has no noteworthy effect on the absorption wavelengths, electron injection (ΔG^{inject}), electronic coupling constants ($|V_{RP}|$) and light harvesting efficiencies (LHE). The electron withdrawing group –COOH lower while electron donating group –OCH_3 increase the energies of highest occupied and lowest unoccupied molecular orbitals. By substituting the –COOH or –OCH_3, we have observed significant effect towards the red shifts in the

absorption spectra. The enhanced ΔG^{inject} and LHE of indole-based squaraine dyes would lead improved short-circuit current density than the referenced sensitizers illuminating former would be proficient dye-sensitized solar cell (DSSCs) materials. The larger values of the reduction potentials of Cis forms than Trans ones showed that open-circuit voltage of former might be superior than later ones. We anticipate that the present investigations would be helpful to design efficient organic sensitizers with enhanced properties.

ACKNOWLEDGEMENTS
This Project was funded by King Abdulaziz City for Science and Technology (KACST) through National Science, Technology and Innovation Plan (NSTIP) under grant number 8-ENE198-3. The authors, therefore, acknowledge with thanks KACST for support for Scientific Research. Also, the authors are thankful to the Deanship of Scientific Research (DSR), King Abdulaziz University for their technical support.

References

1. Y.-K. Lan, C.-I. Huang, *J. Phys. Chem. B* 112 (2008) 14857.
2. R.T. Weitz, K. Amsharov, U. Zschieschang, E.B. Villas, D.K. Goswami, M. Burghard, H. Dosch, M. Jansen, K. Kern, H. Klauk, *J. Am. Chem. Soc.* 130 (2008) 4637.
3. C.R. Newman, C.D. Frisbie, D.A. da Silva Filho, J.-L. Brédas, P.C. Ewbank, K.R. Mann, *Chem. Mater.* 16 (2004) 4436.
4. J. Zaumseil, H. Sirringhaus, *Chem. Rev.* 107 (2007) 1296.
5. H.-Y. Chen, I. Chao, *Chem. Phys. Lett.* 401 (2005) 539.
6. J.O. Escobedo, O. Rusin, S. Lim, R.M. Strongin, *Curr. Opin. Chem. Biol.* 14 (2010) 64.
7. L. Beverina, P. Salice, *Eur. J. Org. Chem.* 2010 (2010) 1207.
8. B. Oswald, L. Patsenker, J. Duschl, H. Szmacinski, O.S. Wolfbeis, E. Terpetschnig, *Bioconjugate Chem.* 10 (1999) 925.
9. H.-G.K. Tatsuo Mori, Teruyoshi Mizutani, Duck-Chool Lee, *Jpn. J. Appl. Phys.* 40 (2001) 5346.
10. G. Chen, H. Sasabe, Y. Sasaki, H. Katagiri, X.-F. Wang, T. Sano, Z. Hong, Y. Yang, J. Kido, *Chem. Mater.* 26 (2014) 1356.
11. F. Silvestri, M.D. Irwin, L. Beverina, A. Facchetti, G.A. Pagani, T.J. Marks, *J. Am. Chem. Soc.* 130 (2008) 17640.
12. D. Bagnis, L. Beverina, H. Huang, F. Silvestri, Y. Yao, H. Yan, G.A. Pagani, T.J. Marks, A. Facchetti, *J. Am. Chem. Soc.* 132 (2010) 4074.
13. L.-N. Yang, Z.-Z. Sun, Q.-S. Li, S.-L. Chen, Z.-S. Li, T.A. Niehaus, *J. Power Sources* 268 (2014) 137.
14. L. Liu, J. Chen, Z. Ku, X. Li, H. Han, *Dyes Pigm.* 106 (2014) 128.
15. G.M. Shivashimpi, S.S. Pandey, R. Watanabe, N. Fujikawa, Y. Ogomi, Y. Yamaguchi, S. Hayase, *J. Photochem. Photobiol., A: Chem.* 273 (2014) 1.
16. L. Beverina, M. Crippa, M. Landenna, R. Ruffo, P. Salice, F. Silvestri, S. Versari, A. Villa, L. Ciaffoni, E. Collini, C. Ferrante, S. Bradamante, C.M. Mari, R. Bozio, G.A. Pagani, *J. Am. Chem. Soc.* 130 (2008) 1894.
17. Y.-S. Yen, H.-H. Chou, Y.-C. Chen, C.-Y. Hsu, J.T. Lin, *J. Mater. Chem.* 22 (2012) 8734.
18. L. Liu, J. Chen, Z. Ku, X. Li, H. Han, *Dyes Pigm.* 106 (2014) 128.
19. G.M. Shivashimpi, S.S. Pandey, R. Watanabe, N. Fujikawa, Y. Ogomi, Y. Yamaguchi, S. Hayase, *J. Photochem. Photobiol., A: Chem.* 273 (2014) 1.

20. C.H. Lee, H.J. Yun, M.R. Jung, J.G. Lee, S.H. Kim, J.H. Kim, *Electrochim. Acta* http://dx.doi.org/10.1016/j.electacta.2014.06.073.
21. G. de Miguel, M. Ziółek, M. Zitnan, J.A. Organero, S.S. Pandey, S. Hayase, A. Douhal, *J. Phys. Chem. C* 116 (2012) 9379.
22. A.G. Al-Sehemi, A. Irfan, A.M. Asiri, Y.A. Ammar, *Spectrochimica Acta Part A: Molecular and Biomolecular Spectroscopy* 91 (2012) 239.
23. A.G. Al-Sehemi, A. Irfan, A.M. Asiri, Y.A. Ammar, *J. Mol. Struct.* 1019 (2012) 130.
24. A. Irfan, N. Hina, A. Al-Sehemi, A. Asiri, *J. Mol. Model.* 18 (2012) 4199.
25. A. Al-Sehemi, A. Irfan, A. Asiri, *Theor. Chem. Acc.* 131 (2012) 1.
26. A. Irfan, A. Al-Sehemi, *J. Mol. Model.* 18 (2012) 4893.
27. A. Irfan, R. Jin, A.G. Al-Sehemi, A.M. Asiri, *Spectrochimica Acta Part A: Molecular and Biomolecular Spectroscopy* 110 (2013) 60.
28. A. Irfan, *Mater. Chem. Phys.* 142 (2013) 238.
29. M. Wiemer, V. Sabnis, H. Yuen, 43.5% efficient lattice matched solar cells, in, 2011, pp. 810804.
30. J. Preat, D. Jacquemin, E.A. Perpète, *Environ. Sci. Technol.* 44 (2010) 5666.
31. D. Liu, R.W. Fessenden, G.L. Hug, P.V. Kamat, *J. Phys. Chem. B* 101 (1997) 2583.
32. B. Burfeindt, T. Hannappel, W. Storck, F. Willig, *J. Phys. Chem.* 100 (1996) 16463.
33. K. Sayama, S. Tsukagoshi, K. Hara, Y. Ohga, A. Shinpou, Y. Abe, S. Suga, H. Arakawa, *J. Phys. Chem. B* 106 (2002) 1363.
34. A. Irfan, *Comp. Mater. Sci.* 81 (2014) 488.
35. A. Irfan, A.G. Al-Sehemi, M.S. Al-Assiri, *J. Fluorine Chem.* 157 (2014) 52.
36. A. Irfan, A.G. Al-Sehemi, M.S. Al-Assiri, *Comp. Theor. Chem* 1031 (2014) 76.
37. A. Irfan, A.G. Al-Sehemi, S. Muhammad, *Synth. Met.* 190 (2014) 27.
38. A.G. Al-Sehemi, A. Irfan, M.A.M. Al-Melfi, A.A. Al-Ghamdi, E. Shalaan, *J. Photochem. Photobiol., A: Chem.* 292 (2014) 1.
39. A.R. Chaudhry, R. Ahmed, A. Irfan, A. Shaari, A.G. Al-Sehemi, *Science of Advanced Materials* 6 (2014) 1727.
40. A.R. Chaudhry, R. Ahmed, A. Irfan, S. Muhammad, A. Shaari, A.G. Al-Sehemi, *Comp. Theor. Chem* 1045 (2014) 123.
41. A.G. Al-Sehemi, A. Irfan, A.M. Asiri, *Chin. Chem. Lett.* 25 (2014) 609.
42. A. Irfan, *J. Theor. Comput. Chem.* 13 (2014) 1450013.
43. A.R. Chaudhry, R. Ahmed, A. Irfan, A. Shaari, H. Maarof, A.G. Al-Sehemi, *Sains Malaysiana* 43 (2014) 867.
44. A. Irfan, A.G. Al-Sehemi, S. Muhammad, *Journal of Quantum Chemistry* 2014 (2014) 6.
45. A. Irfan, *Optik - Intern. J. Light Elect. Optics* 125 (2014) 4825.
46. A. Irfan, A.G. Al-Sehemi, M.S. Al-Assiri, *J. Mol. Graphics Modell.* 44 (2013) 168.
47. R.S. Sánchez-Carrera, V. Coropceanu, D.A. da Silva Filho, R. Friedlein, W. Osikowicz, R. Murdey, C. Suess, W.R. Salaneck, J.-L. Brédas, *J. Phys. Chem. B* 110 (2006) 18904.
48. B.M. Wong, J.G. Cordaro, *J. Chem. Phys.* 129 (2008).
49. A. Irfan, A.G. Al-Sehemi, A. Kalam, *J. Mol. Struct.* 1049 (2013) 198.
50. D. Guillaumont, S. Nakamura, *Dyes Pigm.* 46 (2000) 85.
51. C. Zhang, W. Liang, H. Chen, Y. Chen, Z. Wei, Y. Wu, *J. Mol. Struct. (TheoChem)* 862 (2008) 98.
52. A. Irfan, R. Cui, J. Zhang, L. Hao, *Chem. Phys.* 364 (2009) 39.
53. A. Al-Sehemi, A. Irfan, A. Asiri, *Theor. Chem. Acc.* 131 (2012) 1199.
54. A. Al-Sehemi, M. Al-Melfi, A. Irfan, *Struct. Chem.* 24 (2013) 499.
55. R. Jin, A. Irfan, *Comp. Theor. Chem* 986 (2012) 93.
56. A.G. Al-Sehemi, A. Irfan, A.M. El-Agrody, *J. Mol. Struct.* 1018 (2012) 171.
57. A. Irfan, F. Ijaz, A.G. Al-Sehemi, A.M. Asiri, *J. Comput. Electron.* (2012) 1.
58. J. Preat, C. Michaux, D. Jacquemin, E.A. Perpète, *J. Phys. Chem. C* 113 (2009) 16821.
59. V.T.T. Huong, H.T. Nguyen, T.B. Tai, M.T. Nguyen, *J. Phys. Chem. C* 117 (2013) 10175.

60. G. Scalmani, M.J. Frisch, B. Mennucci, J. Tomasi, R. Cammi, V. Barone, *J. Chem. Phys.* 124 (2006) 094107.
61. D. Matthews, P. Infelta, M. Grätzel, *Sol. Energy Mater. Sol. Cells* 44 (1996) 119.
62. G. Pourtois, D. Beljonne, J. Cornil, M.A. Ratner, J.L. Brédas, *J. Am. Chem. Soc.* 124 (2002) 4436.
63. C.-P. Hsu, *Acc. Chem. Res.* 42 (2009) 509.
64. R.A. Marcus, *Reviews of Modern Physics* 65 (1993) 599.
65. M. Hilgendorff, V. Sundström, *J. Phys. Chem. B* 102 (1998) 10505.
66. J. Asbury, Y.-Q. Wang, E. Hao, H. Ghosh, T. Lian, *Res. Chem. Intermed.* 27 (2001) 393.
67. R. Katoh, A. Furube, T. Yoshihara, K. Hara, G. Fujihashi, S. Takano, S. Murata, H. Arakawa, M. Tachiya, *J. Phys. Chem. B* 108 (2004) 4818.
68. A. Hagfeldt, M. Graetzel, *Chem. Rev.* 95 (1995) 49.
69. P.F. Barbara, T.J. Meyer, M.A. Ratner, *J. Phys. Chem.* 100 (1996) 13148.
70. S.F.a.A.S. Filippo De Angelis, *Nanotechnology* 19 (2008) 424002.
71. G. Benkö, J. Kallioinen, J.E.I. Korppi-Tommola, A.P. Yartsev, V. Sundström, *J. Am. Chem. Soc.* 124 (2001) 489.
72. S. Iwai, K. Hara, S. Murata, R. Katoh, H. Sugihara, H. Arakawa, *J. Chem. Phys.* 113 (2000) 3366.
73. H.S. Nalwa, in, Handbook of advanced electronic and photonic materials and devices, Academic: San Diego CA, 2001.
74. M. Cassida, in, recent Advances in density Functional Methods: Time dependent density functional response Theory for molecules, DP Chong: Singapore, 1995.
75. M.D.B. D.C. Harris, in, Symmetry and Spectroscopy, Dover: New York US, 1998.
76. J. Zhang, Y.-H. Kan, H.-B. Li, Y. Geng, Y. Wu, Y.-A. Duan, Z.-M. Su, *J. Mol. Model.* 19 (2013) 1597.
77. N. Robertson, *Angew. Chem. Int. Ed.* 45 (2006) 2338.
78. A.G. Al-Sehemi, A. Irfan, A.M. Fouda, *Spectrochimica Acta Part A: Molecular and Biomolecular Spectroscopy* 111 (2013) 223.
79. C.J. Brabec, A. Cravino, D. Meissner, N.S. Sariciftci, T. Fromherz, M.T. Rispens, L. Sanchez, J.C. Hummelen, *Adv. Funct. Mater.* 11 (2001) 374.